Sensors and Materials, Vol. 35, No. 11 (2023) 3551–3565
MYU Tokyo

S & M 3435

Investigation into Ethanol Concentration Changes of Ethanol–Water Solution Using Polarization Property Associated with Surface Plasmon Resonance in Aluminum Grating in Conical Mounting

Toyonori Matsuda,[1*] Hiroyuki Odagawa,[1] Isao Tsunoda,[1]
Masanori Nagata,[2] and Takao Kawakita[2]

[1]Institute of National College of Technology, Kumamoto Campus, 2659-2 Suya, Koshi, Kumamoto 861-1102, Japan
[2]Kumabou Metal Co., Ltd., 1-4-15 Nagamine-West, Higashi-Ward, Kumamoto 861-8037, Japan

(Received August 16, 2023; accepted October 10, 2023)

Keywords: surface plasmon resonance, metal grating, conical mounting, Stokes parameters, ethanol concentration

We experimentally investigated the changes in the ethanol concentration of an ethanol–water solution using a polarization property of the (specularly) reflected light associated with surface plasmon resonance (SPR) occurring in an aluminum diffraction grating in a conical mounting. The polarization property, which is observed as a rapid change in the normalized Stokes parameter s_3 of the reflected light, can be successfully applied to refractive index sensing: the zero-crossing point of s_3 precisely and easily determines the resonance angle θ_{sp} at which SPR occurs; s_3 in the vicinity of θ_{sp} varies largely in response to a small change in the refractive index of a sample. Using the features of the rapid change in s_3, we examined the ethanol concentration changes over a wide range from 0 to 100 percent by weight (wt%) through the measurement of θ_{sp}. Furthermore, we detected a small amount of ethanol component in water through the measurement of s_3 under the angle of incidence fixed at the resonance angle of pure water.

1. Introduction

Surface plasmon resonance (SPR)[(1)] is associated with the excitation of surface plasmons along a metal–dielectric interface by an optical beam, and the occurrence of SPR causes abrupt changes in both the intensity[(2)] and phase[(3)] of the reflected light. As the occurrence conditions of SPR strongly depend on the refractive index of the material on the metal surface, SPR can be used for refractive index sensing,[(4)] and a variety of SPR-based sensors have been extensively developed in many fields including biosensing and chemical analysis.[(5,6)] The most widely used SPR sensors are based on a change in the level of intensity of the reflected light. Such intensity-change-based SPR sensors have a fundamentally straightforward optical configuration since a

*Corresponding author: e-mail: tmatsu@kumamoto-nct.ac.jp
https://doi.org/10.18494/SAM4611

ISSN 0914-4935
https://myukk.org/

photodetector directly measures the intensity of the reflected light. On the other hand, SPR sensors based on the phase shifts or polarization properties of the reflected light have been studied.[7–9] The utilization of such phase information has achieved significant improvements in SPR sensing, such as an extremely high sensitivity,[10] since the phase of the reflected light markedly changes in response to the occurrence of SPR compared with the intensity of the reflected light. However, phase-change-based SPR sensors generally require a complex optical configuration for phase detection techniques in comparison with that of intensity-change-based SPR sensors. Accordingly, the simplification or miniaturization of SPR sensing techniques based on the phase information has been a promising development issue.[9] The simplified and miniaturized design of SPR sensors has been attracting attention for a wide variety of applications[11] such as portable sensor systems,[12] in-line measurement,[13] and smartphone-platform SPR sensors.[14]

Matsuda and Odagawa have reported a technique of refractive index sensing by using a polarization property of the (specularly) reflected light, or the zeroth-order diffracted light, when SPR occurs in a metal grating.[15] To simply and sensitively detect the occurrence of SPR in a metal grating, they used a conical mounting in which the plane of incidence is not perpendicular to the grooves of the metal grating, while a metal grating is commonly used in a planar mounting, in which the plane of incidence is perpendicular to the grooves. SPR occurring in a metal grating in a conical mounting has long been investigated[16–20] and has interesting features for refractive index sensing.[18–20] In particular, the polarization property of the reflected light is attractive:[15] when a metal grating in a conical mounting is illuminated by *p*-polarized light whose electric field is parallel to the plane of incidence, the reflected light changes rapidly from right- (or left-) to left- (or right-) elliptical polarization via linear polarization at the resonance angle θ_{sp} at which SPR occurs. The polarization property is observed as a rapid change in the normalized Stokes parameter s_3, which indicates the intensity difference between the right- and left-circularly polarized components. The rapid change in s_3 at around θ_{sp} has features that are successfully applied to SPR sensing: θ_{sp} is precisely and easily determined as the zero-crossing point on the s_3 curve (the incident angle dependence of s_3) and, furthermore, s_3 in the vicinity of θ_{sp} varies largely with a small change in the refractive index of the sample. The effectiveness of the rapid change in s_3 in SPR sensing has been indicated through an experiment on detecting the refractive index change of samples of H_2, O_2, N_2, and CO_2 gases.[15] The SPR sensing technique using the rapid change in s_3 is potentially implemented with a relatively straightforward optical configuration that fundamentally consists of a metal grating in a conical mounting, a light source part, and a light-receiving part for the measurement of s_3.

In this study, we applied the SPR sensing technique using the rapid change in s_3 to the detection of a change in the ethanol concentration of an ethanol–water solution. Many studies have already been conducted on measurements of the ethanol concentration of an ethanol–water solution through SPR sensing techniques.[21–25] Ethanol has a wide range of uses across various industries, and there are many demands on the measurement of ethanol content for process monitoring or quality assurance in the production of products using ethanol.[26] We considered an optical configuration in which pure water or an ethanol–water solution is set on the surface of an aluminum diffraction grating in a conical mounting as a liquid sample. We then observed a

rapid change in s_3 that has an approximately linear portion with a steep slope in the vicinity of the resonance angle θ_{sp}. The steep slope of the approximately linear portion in the rapid change in s_3, which means the occurrence of sharp SPR,[15] enables us to detect sensitively a change in the ethanol concentration of an ethanol–water solution. We examined ethanol concentration changes over a wide range through the measurement of θ_{sp}, which is simply and accurately obtained as the zero-crossing point in the rapid change in s_3 for ethanol–water solutions with various ethanol concentrations from 0 to 100 percent by weight (wt%). Furthermore, we detected a small amount of ethanol in water through the measurement of s_3 under the angle of incidence fixed at θ_{sp} for pure water. The detection technique, which is based on the large variation of s_3 in the vicinity of θ_{sp}, is applied to the detection of ethanol concentration that slightly changes from a certain reference value.

2. Preparation for Experiment

2.1 Aluminum grating in conical mounting and optical configuration

Here, we explain the optical configuration of an aluminum grating in a conical mounting, on the surface of which an ethanol–water solution or pure water is set as a liquid sample. Figure 1 shows a schematic of an aluminum grating in a conical mounting. We determined the *XYZ*-coordinate system as follows: the aluminum grating is periodic with period d in the X direction and uniform in the Y direction, and the grating normal is coincident with the Z axis. The aluminum grating is arranged in a conical mounting such that the plane of incidence makes an angle of ϕ with the X axis. The angle ϕ is hereinafter referred to as the azimuthal angle, and the

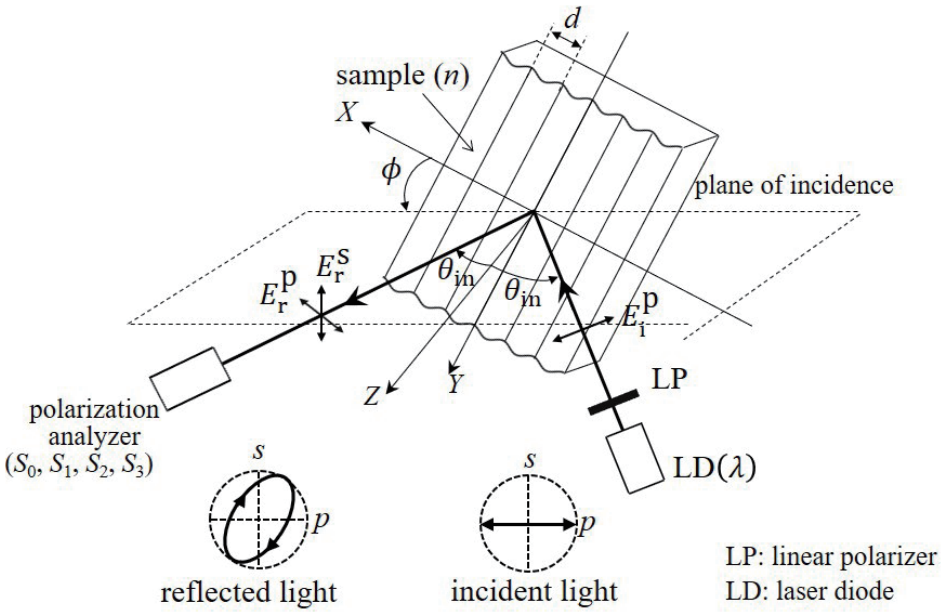

Fig. 1. Optical configuration for detection of ethanol concentration change of an ethanol–water solution through SPR in aluminum grating in conical mounting.

conical mounting is specified by a nonzero ϕ. The front area of the grating surface is filled with the liquid sample with refractive index n. A light beam of wavelength λ from a laser diode (LD) becomes p-polarized after passing through a linear polarizer whose transmission axis is parallel to the plane of incidence and the p-polarized light is then illuminated on the surface of the aluminum grating at the angle of incidence θ_{in} measured from the Z axis.

We focused on the polarization property of the reflected light, i.e., the zeroth-order diffracted light, from the aluminum grating in the conical mounting. When p-polarized light is illuminated on the aluminum grating in the conical mounting, the reflected light has an s-component in which an electric field is perpendicular to the plane of incidence, in addition to a p-component. [19] Therefore, the reflected light becomes elliptically polarized for the p-polarized incidence, as illustrated in Fig. 1. As the quantity for the detection of a change in ethanol concentration of ethanol–water solutions, we employ the Stokes parameter normalized by the intensity of the reflected light I_r:

$$s_3 = \frac{S_3}{I_r} = 2\frac{E_r^s / E_r^p}{1+\left(E_r^s / E_r^p\right)^2}\sin\delta. \tag{1}$$

Here, E_r^p and E_r^p respectively are the amplitudes of the p and s components of the electric field of the reflected light, and δ (= $\delta_s - \delta_p$) is the phase difference between them. The normalized Stokes parameter s_3 is also expressed as $s_3 = (I_R - I_L)/(I_R + I_L)$ with I_R and I_L respectively being the intensities of the right- and left-circularly polarized components of the reflected light. Thus, s_3 means the difference in intensity between the right- and left-circularly polarized components, and varies from 1 (right-circular polarization) to −1 (left-circular polarization) via 0 (linear polarization). From the measured values of Stokes parameters S_0 to S_3, we evaluated the phase difference δ and the amplitude ratio E_r^s / E_r^p to examine the behavior of the p and s components associated with SPR.

In this study, we considered SPR when only the zeroth-order diffracted mode propagates and the TM component of the −1st-order evanescent mode in the diffracted light couples with surface plasmons that propagate along the interface between the liquid sample and the grating surface. Here, TM means that the relevant magnetic field is transverse to the Z axis in Fig. 1. In the optical configuration of Fig. 1, the zeroth-order diffracted mode only propagates when the following relation is satisfied for $m = -1$:

$$\hat{\alpha}_m^2 + \hat{\beta}^2 > n\,, \tag{2}$$

where $\hat{\alpha}_m = n\sin\theta_{in}\cos\phi + m\frac{\lambda}{d}$ and $\hat{\beta}_m = n\sin\theta_{in}\sin\phi$ respectively are the propagation constants in the X and Y directions of the mth-order evanescent mode normalized by the wave number of incident light. We chose the grating period d (= 417 nm) and the wavelength of incident light λ (= 672 nm) in the experimental setup described below so that Eq. (2) is satisfied. In a metal grating, SPR occurs when a phase matching condition is satisfied, i.e., the wave vector

of an evanescent mode in the diffracted light coincides with that of surface plasmons.[27] The phase matching condition for the occurrence of SPR in the optical configuration of Fig. 1 is expressed as

$$\left(\mathrm{Re}\left[\hat{k}_{sp}\right]\right)^2 = \hat{\alpha}_{-1}^2 + \hat{\beta}^2 . \tag{3}$$

Here, $\hat{k}_{sp}$ is the propagation constant of the surface plasmon wave normalized by the wave number of the incident light and Re[ ] denotes the real part of the complex number. Therefore, if the wavelength of incident light λ and the grating period d are kept constant, the occurrence of SPR is determined by the refractive index of the liquid sample n, the angle of incidence θ_{in}, and the azimuthal angle ϕ.

2.2 Experimental setup and ethanol–water solution preparation

Figure 2(a) shows a view of the experimental setup with the optical configuration illustrated in Fig. 1. As an aluminum grating, we used a commercially available aluminum diffraction

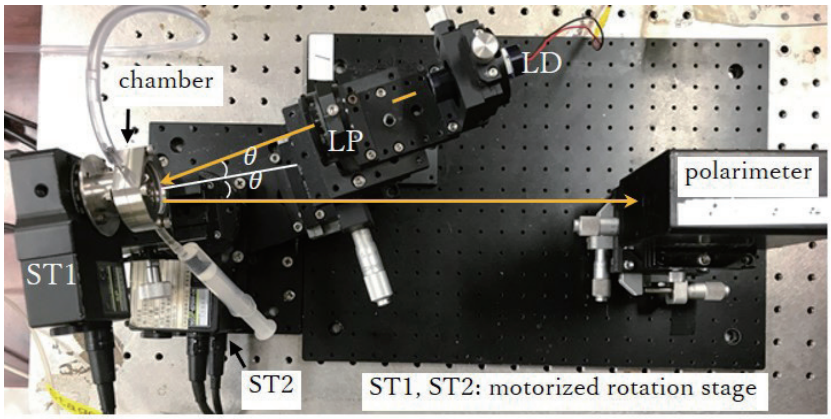

(a)

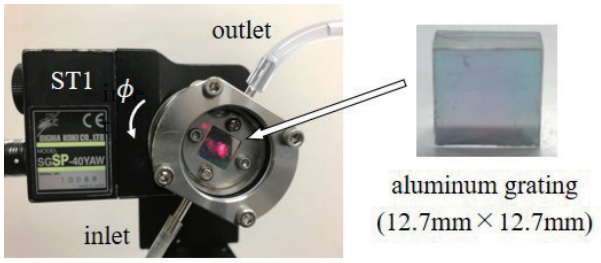

(b)

Fig. 2. (Color online) Experimental setup for investigation of ethanol concentration changes of an ethanol–water solution through SPR in aluminum grating in conical mounting: (a) full view of experimental setup and (b) aluminum grating and chamber with embedded aluminum grating.

grating (Stock number #43-776, Edmund Optics Japan) with a groove density of 2400 lines/nm (period d = 417 nm). The aluminum grating has no antioxidant films, but a natural aluminum oxide film is formed on its surface. We arranged the aluminum grating in a chamber that can be rotated about its central axis to set an azimuthal angle ϕ using the motorized rotation stage (ST1), as shown in Fig. 2(b). A light beam of wavelength λ = 672 nm from an LD module (Stock number #38-922, Edmund Optics Japan) becomes p-polarized after passing through a linear polarizer whose transmission axis is parallel to the plane of incidence. The elliptical spot size of the laser beam is 5 × 2 mm and the power is 2 mW. The p-polarized light is illuminated on a glass window of the chamber at an angle θ measured from the normal to the glass window and is then incident on the surface of the aluminum grating through a liquid sample such as pure water or ethanol–water solution. The reflected light from the aluminum grating is extracted through the glass window after passing through the liquid sample. The Stokes parameters S_0 to S_3 of the reflected light are measured using a PAX1000VIS polarimeter (Thorlabs, Inc.). In the experimental setup, we rotated θ using the motorized rotation stage (ST2) to vary the angle of incidence on the grating surface θ_{in} illustrated in Fig. 1. We therefore refer to θ as the angle of incidence hereinafter. The relationship between θ_{in} and θ is given by Snell's law as $n_{air}\sin\theta = n\sin\theta_{in}$ with n_{air} and n respectively being the refractive indices of air and a liquid sample.

We prepared an ethanol–water solution from pure water of 1 MΩcm electric resistivity and ethanol (99.5) (cat. no. 057-0045, FUJIFILM Wako Pure Chemical Corporation), which is an ethanol reagent with the tested concentration of 100.0 wt%. We mixed ethanol (99.5) of W_1 (g) and pure water of W_0 (g), and the ethanol concentration of the mixture is denoted by C (wt%), which is the weight percent concentration of the ethanol–water solution given by

$$C = \frac{W_1}{W_1 + W_0} \times 100 \ (\text{wt\%}). \tag{4}$$

Here, C = 0 and 100 wt% respectively represent the pure water and the ethanol reagent. We manually injected the ethanol–water solution into the chamber from the inlet with a syringe, as shown in Fig. 2(a). The experiment was performed in a laboratory without temperature control for the ethanol–water solutions.

3. Experimental Results and Discussion

In this section, we report the experimental data obtained with the experimental setup described in Sect. 2. As a result, a rapid change in s_3 with a steep slope in the vicinity of θ_{sp} is obtained, and this rapid change is then indicated to be applicable in the investigation of the changes in the ethanol concentration of an ethanol–water solution.

3.1 Rapid change in s_3 associated with SPR

We first explain the polarization property of the reflected light from the aluminum grating in the conical mounting in the experimental setup shown in Fig. 2. The pure water of C = 0 wt% is

used as a liquid sample in the experimental results indicated in this subsection. Figure 3(a) shows I_r and s_3 of the reflected light from the aluminum grating in the conical mounting with the azimuthal angle set to ϕ = 10° when θ (the angle of incidence on the glass window of the chamber) is varied from 8° to 18° at intervals of 0.025°. As the cut-off for the −1st-order diffracted mode corresponds to $\theta = \theta_{-1}$ (= 16.625°) in Fig. 3(a), only the zeroth-order diffracted mode propagates and the other diffracted modes are evanescent in the range of θ less than θ_{-1}. We observe the partial absorption of incident light as a dip at θ_A = 12.100° in the I_r curve. The absorption dip is caused by SPR in which surface plasmons propagating along the interface between the pure water and the grating surface couple with the TM component of the –1st-order evanescent mode in the diffracted light.[27]

On the other hand, s_3 becomes zero at θ_{sp} = 12.069°, which is very close to θ_A, and largely varies from a positive maximum value to a negative minimum value within a narrow range of θ. The rapid change in s_3 at around θ_{sp} means that the reflected light becomes linearly polarized at θ_{sp} and rapidly changes from right-circularly polarized to left-circularly polarized around θ_{sp}. The rapid change in s_3 as well as the absorption dip of I_r, is associated with the excitation of surface plasmons in the aluminum grating in the conical mounting.[15] The occurrence process of the rapid change in s_3 can be clarified from the behaviors of δ (phase difference between the p and s components of the reflected light) and E_r^s / E_r^p (their amplitude ratio) when SPR occurs: as shown in Fig. 3(b), δ = 180° provides θ_{sp} at which s_3 becomes zero and δ rapidly changes from 90° to 270° via 180° at θ_{sp}, and E_r^s / E_r^p takes a peak value at the angle of incidence very close to θ_{sp}. The 180° phase shift of δ and the increase in E_r^s / E_r^p at around θ_{sp} result in the rapid change in s_3, as expected from Eq. (1). The resonance behaviors of δ and E_r^s / E_r^p are strongly affected by SPR, and thus the rapid change in s_3 reacts sensitively to a change in the occurrence condition of SPR, such as a refractive index change of a liquid sample. The zero-crossing point on the s_3 curve (θ_{sp}) is not always coincident with the angle of incidence at the absorption dip (θ_A), but they are very close to each other.[15] Hence, we employ the zero-crossing point θ_{sp} as the resonance angle at which SPR occurs in a metal grating in a conical mounting. The resonance

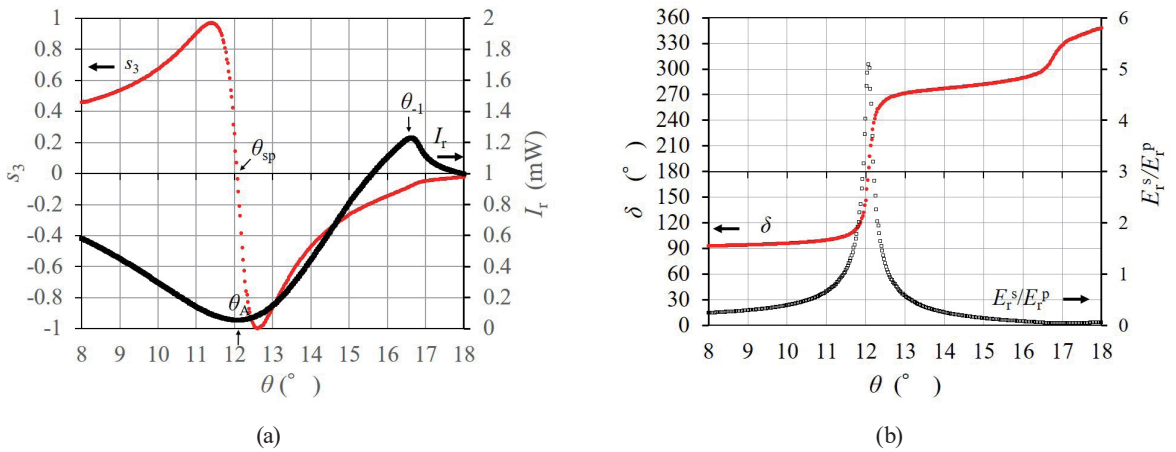

Fig. 3. (Color online) Polarization property of reflected light associated with SPR in aluminum grating in conical mounting with ϕ = 10°: (a) s_3 and I_r ; (b) δ and E_r^s / E_r^p. Liquid sample is pure water of C = 0 wt%.

angle θ_{sp} is precisely and easily determined through zero-crossing point detection since the $s_3$curve is approximately linear around θ_{sp}. In practice, the detection of θ_{sp} can be implemented regardless of the sharpness of SPR even when the absorption dip in the I_r curve is shallow and broad.

We next describe the determination of the azimuthal angle ϕ in a conical mounting. Figure 4 shows s_3 as a function of θ for ϕ = 0°, 15°, 20°, and 30°, in addition to that for ϕ = 10° in Fig. 3(a). As ϕ is one of the parameters that determine the occurrence of SPR, ϕ has an effect on the behavior of the rapid change in s_3. The resonance angle θ_{sp} varies with ϕ, and the slope of the approximately linear portion of the s_3 curve in the vicinity of θ_{sp} is affected by ϕ. The slope in the rapid change in s_3, which corresponds to the sharpness of SPR,[15] is related to the sensitivity in the detection of a change in the refractive index of a liquid sample. Consequently, s_3 in the vicinity of θ_{sp} varies largely in response to a small refractive index change when the slope in the rapid change in s_3 increases. In the experiment described below, we therefore use ϕ = 10° since the rapid change in s_3 has the steepest slope around the resonance angle.

3.2 Effect of ethanol concentration on resonance angle θ_{sp}

We investigated the ethanol concentration change of an ethanol–water solution using the rapid change in s_3 explained in Sect. 3.1. We prepared fifteen samples of ethanol–water solutions with different ethanol concentrations from C = 0 to 100 wt%. We then measured the refractive index n_D and temperature T °C of the prepared ethanol–water solutions with a digital refractometer PR-RI (cat. no. 3480, ATAGO CO., LTD.). While n_D is the refractive index for D line (wavelength 589 nm), which is different from 672 nm of the experiment in this paper, we took n_D as a reference for considering the effect of the ethanol concentration of the ethanol–water solutions on their refractive index. No temperature correction was made for the measured values of n_D. The ethanol concentration, refractive index, and temperature of the prepared ethanol–water solutions are listed in Table 1.

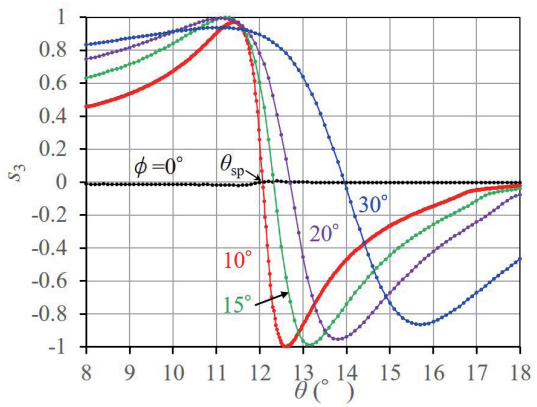

Fig. 4. (Color online) s_3 curves for several ϕ values. Parameters other than ϕ are the same as those in Fig. 3. No rapid change in s_3 appears for ϕ = 0°, which is not conical mounting.

Table 1
θ_{sp} and θ_A for various C's from 0 to 100 wt%.

C (wt%)*	θ_{sp} (°)	θ_A (°)	n_D	T (°C)
0.00	12.069	12.100	1.3329	20.8
10.00	11.468	11.500	1.3391	21.8
20.01	10.931	10.975	1.3463	20.9
29.98	10.511	10.550	1.3526	20.1
39.95	10.182	10.200	1.3571	20.3
49.99	9.949	9.950	1.3600	21.0
59.92	9.808	9.825	1.3627	20.2
64.98	9.728	9.750	1.3635	20.1
70.01	9.652	9.650	1.3640	20.0
74.82	9.623	9.650	1.3646	19.2
79.94	9.604	9.625	1.3650	18.7
85.00	9.601	9.625	1.3650	18.4
89.96	9.644	9.650	1.3642	18.6
94.97	9.683	9.700	1.3640	18.7
100.00	9.829	9.850	1.3616	18.6

*Value calculated from Eq. (4).

We performed measurements for s_3 and I_r when θ was varied from 9° to 12° (or 13°) at intervals of 0.025° with the azimuthal angle set to $\phi = 10°$ for each sample of the fifteen ethanol–water solutions. Figure 5(a) shows the s_3 curves for the fifteen ethanol–water solutions with ethanol concentrations from $C = 0$ to 100 wt%. Each s_3 curve exhibits a rapid change in s_3 that has approximately the same slope in the vicinity of the zero-crossing point θ_{sp}, and the rapid change in s_3 follows the variation of C. The behavior of the rapid change in s_3 indicates the effect of the change in C on SPR. Figure 5(b), which is the enlargement of the rectangular region (b) in Fig. 5(a), shows the rapid change in s_3 in the vicinity of θ_{sp} for C larger than 40 wt%. We demonstrate that θ_{sp} can be obtained by zero-crossing point detection in the approximately linear portion for all the values of C. We also observe in Fig. 5(b) that the rapid change in s_3 shifts to the low-incident-angle side with an increase in C and returns to the high-incident-angle side over certain concentrations slightly above 80 wt%. Accordingly, the rapid change in s_3 can be nearly the same for two different concentrations before and after the critical value, such as 80 and 85 wt%.

Figure 5(c) shows the I_r curves corresponding to the s_3 curves in Fig. 5(a), and the absorption dips in the I_r curves for high ethanol concentrations are enlarged in Fig. 5(d). The variation of θ_A at which I_r becomes minimum in the absorption dip also indicates the effect of C on SPR since θ_A is very close to θ_{sp} for the respective C's, as shown in Table 1. However, the rapid change in s_3 clearly indicates the effect of C on SPR in comparison with the absorption dip and thus allows for the more accurate examination of the ethanol concentration change. In particular, the zero-crossing point of s_3 definitely and easily determines the occurrence of SPR even for the ethanol–water solutions with high ethanol concentrations in which the absorption dips are very close together.

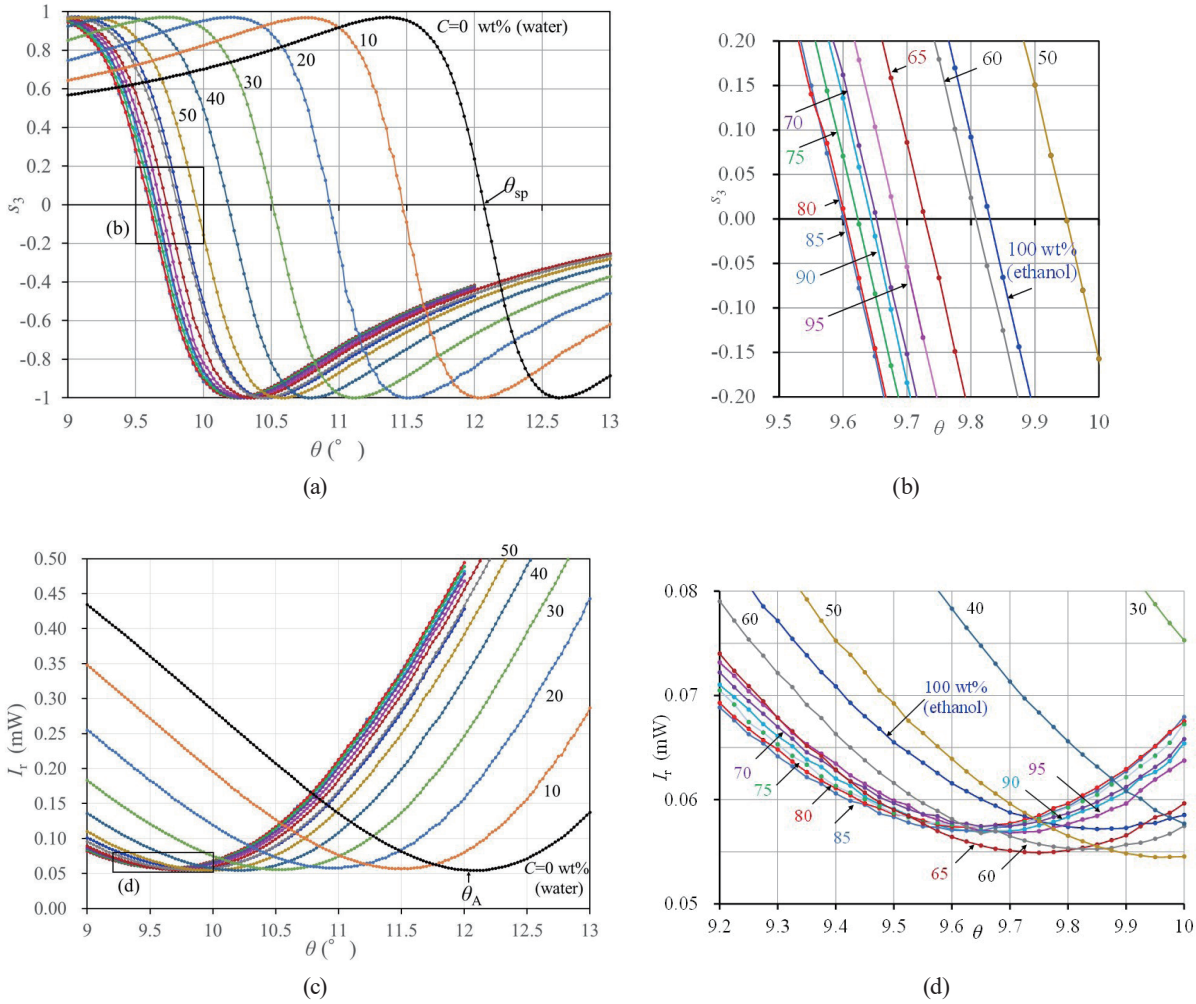

Fig. 5. (Color online) SPR properties for ethanol–water solutions with various ethanol concentrations from $C = 0$ to 100 wt%: (a) s_3 as a function of θ, (b) enlargement of rectangular region in Fig. 5(a), (c) I_r as a function of θ, and (d) enlargement of rectangular region in Fig. 5(c). Parameters other than C are the same as those in Fig. 3.

Here, we discuss the relationship between C and θ_{sp} obtained from the s_3 curves. We show θ_{sp} as a function of C from 0 to 100 wt% in Fig. 6, in which n_D for each C is also plotted on a reverse scale. The values of C, θ_{sp}, and n_D in Fig. 6 are taken from Table 1. The dependence of the ethanol concentration of an ethanol–water solution on its refractive index is described in many publications,[28–30] including studies based on SPR:[23,24] the refractive index monotonically increases with increasing ethanol concentration from 0 wt% to a critical value near 80 wt%, but the refractive index decreases with increasing ethanol concentration over the critical value. As indicated in Fig. 6, the variation of n_D with C exhibits the ethanol concentration dependence of refractive index described in the literature. We observe in Fig. 6 that the variation of θ_{sp} with respect to C is similar to that of n_D. This implies that θ_{sp} varies in response to the refractive index change of an ethanol–water solution accompanying the change in C. Thus, the

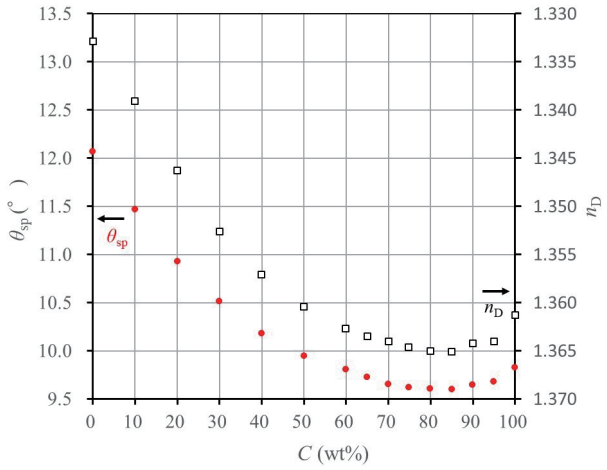

Fig. 6. (Color online) θ_{sp} and n_D as functions of C ranging from 0 to 100 wt%. n_D is plotted on reverse scale. The values of C, θ_{sp}, and n_D are taken from Table 1.

measurement of θ_{sp} leads to the detection of the ethanol concentration change of ethanol–water solutions, whereas the nonlinearity between θ_{sp} and C, including the quadratic response in the high concentration range, needs to be considered.(29)

3.3 Detection of small ethanol concentration change

We describe the detection of a small ethanol concentration change from a certain reference value of ethanol concentration using the approximate linearity of s_3 in the vicinity of θ_{sp}. If the ethanol concentration change ΔC is very small, the shift of the resonance angle $\Delta\theta_{sp}$ also becomes small, and thus it can be difficult to measure $\Delta\theta_{sp}$ with high accuracy. As an alternative technique for measuring such a small shift of the resonance angle, an efficient technique is proposed.(15) Figure 7 shows the measurement technique for detecting a small ethanol concentration change ΔC from C wt% of pure water. We first measure the rapid change in s_3 (solid curve) for the pure water and then determine the resonance angle θ_{H_2O}. Under the optical configuration with the fixed angle of incidence at θ_{H_2O}, if C changes by ΔC from 0 wt%, s_3 linearly varies from 0 to Δs_3 accompanying the shift of the rapid change in s_3 (broken curve), as illustrated in Fig. 7. Consequently, we can estimate a small change in ethanol concentration, ΔC, through the measurement of Δs_3 without measuring $\Delta\theta_{sp}$.

We performed an experiment on the detection of a small amount of ethanol component in water by the measurement technique stated above. We prepared nine samples of ethanol–water solutions with different ethanol concentrations from C = 0.1 to 5 wt%. We determined θ_{H_2O} = 11.40° as the zero-crossing point on the s_3 curve for pure water. The state in which the chamber is filled with pure water and the angle of incidence θ is fixed at θ_{H_2O} is referred to here as the initial state. Figure 8 shows the time responses of s_3 when each sample of the nine ethanol–water solutions is manually injected into the chamber with a syringe at t = 10 s after the initial

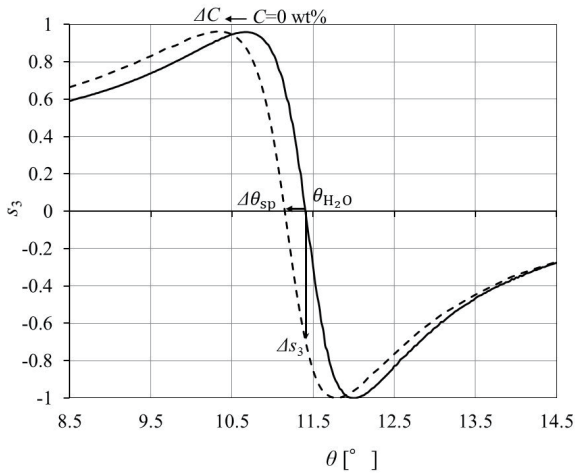

Fig. 7. Measurement technique for detection of a small amount of ethanol component in water using approximate linearity of s_3 in vicinity of resonance angle of pure water θ_{H_2O}.

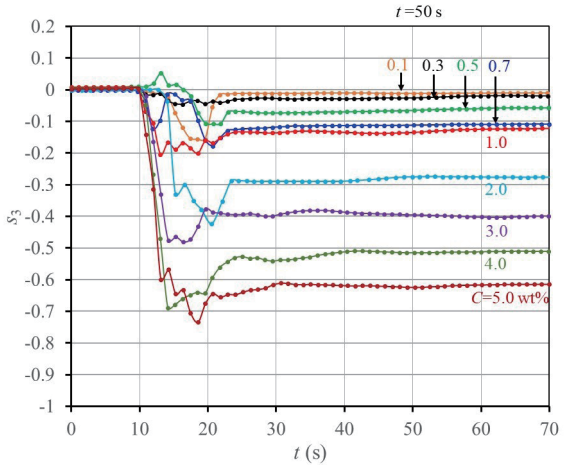

Fig. 8. (Color online) Time responses of s_3 for nine ethanol–water solutions with ethanol concentrations from C = 0.1 to 5 wt%.

state. It takes twenty to thirty seconds from the start of injection to the stabilization of s_3 because of the spatially and temporally heterogeneous distributions of the ethanol–water solutions in the chamber due to manual injection. Also, the values of s_3 in the initial state for the respective ethanol–water solutions deviate from zero owing to drift. Drift is a slow and small variation in s_3, but it cannot be ignored in the measurement of low-level signals. Therefore, we used the difference between the stable and initial values of s_3 as the signal output Δs_3 to determine the ethanol concentration change. Figure 9 shows Δs_3 obtained from the values of s_3 at t = 50 s (stable value) and 10 s (initial value) in the time response for the respective samples from C = 0.1 to 5 wt%. We observed a linear variation in Δs_3 with C, in which the R squared

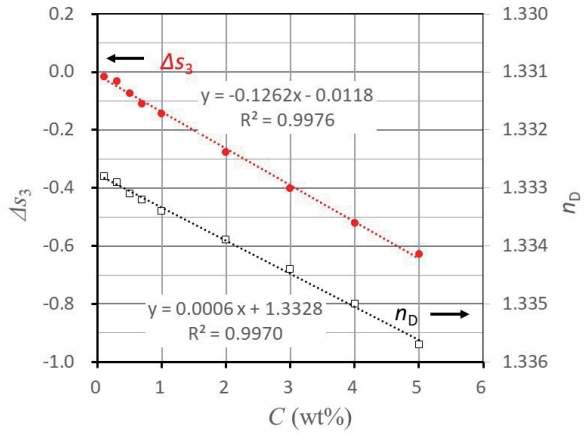

Fig. 9. (Color online) Signal output Δs_3 and n_D as functions of C. Δs_3 is obtained as the difference between s_3 at t = 50 s and that at 10 s in respective time response curves of s_3 in Fig. 8. n_D is plotted on a reverse scale.

value in linear regression is 0.9976. Consequently, the measurement of Δs_3 allows for the detection of a small ethanol concentration change within a range of low ethanol concentrations. The linear variation of Δs_3 with C is based on the fact that the refractive index of the ethanol–water solution is linearly dependent on the ethanol concentration in the low ethanol concentration range.[29] As confirmed in Fig. 9, n_D indicates a linear dependence on C.

We mention here the sensitivity in the detection of the ethanol concentration change in a low concentration range from the calibration curve of Δs_3 versus C in Fig. 9. The ethanol concentration resolution is calculated as $\sigma_C = |K|^{-1} \sigma_{system}$ (wt%), where K (1/wt%) is the slope of the calibration curve and σ_{system} is the s_3 resolution in the optical system of the experimental setup.[7] If the s_3 resolution is assumed to be $\sigma_{system} = 10^{-3}$, the ethanol concentration resolution is calculated as $\sigma_C = 0.0079$ wt% with $K = -0.1262$ 1/wt%. We also infer from Δs_3 and n_D in Fig. 9 that the variations in the fifth decimal place of refractive index will be detected under $\sigma_{system} = 10^{-3}$. Higher sensitivity is achieved by increasing the slope of the approximately linear portion in the rapid change in s_3 as it mainly determines K. As already indicated in Fig. 4, the azimuthal angle in a conical mounting $\phi = 10°$ provides the steepest slope of the rapid change in s_3 in the experiment in this paper, resulting in the higher sensitivity.

In consideration of the above, the use of the rapid change in s_3 allows for the detection of the ethanol concentration change of an ethanol–water solution. Furthermore, there are some issues for the application of the rapid change in s_3 to more accurate and stable measurements of ethanol concentration. As shown in Fig. 8, the time response of s_3 is slow and unstable when the ethanol–water solution is manually injected to the chamber with a syringe. An improvement in the flow pass system of a liquid sample in the experimental setup is needed to accurately investigate the response time or stability of the detection signal in the measurement technique using the rapid change in s_3. Also, temperature compensation for the detection signal is needed to achieve highly accurate measurements of ethanol concentration or concentration measurements over a wide temperature range.[30]

4. Conclusions

We have experimentally investigated the change in ethanol concentration of an ethanol–water solution using the rapid change in s_3, which is associated with SPR occurring in an aluminum grating in a conical mounting. As a result, we demonstrated that the rapid change in s_3 is successfully applied to the examination of the ethanol concentration change of an ethanol–water solution: the ethanol concentration change is examined in a wide dynamic range from the measurement of θ_{sp}; the ethanol concentration that slightly deviates from a certain reference value is simply and sensitively detected from the measurement of s_3 under the fixed angle of incidence. The experimental results presented suggest that the rapid change in s_3 can be applicable for the refractive index sensing of liquid samples other than ethanol–water solutions. Also, the utilization of the rapid change in s_3 can be promising for the simplification or miniaturization of an SPR sensing technique based on polarization information, as s_3 is measured in a relatively straightforward optical configuration with a metal grating in a conical mounting.

Acknowledgments

The authors sincerely thank Mr. Toshio Kobayashi for his helpful cooperation and valuable guidance in the experiment in this study.

References

1 H. Raether: Surface Plasmons on Smooth and Rough Surfaces and on Gratings (Springer-Verlag, Berlin Heidelberg, New York, 1988) Chaps. 1 and 6. https://doi.org/10.1007/BFb0048317
2 R. W. Wood: Proc. Phys. Soc. London **18** (1902) 269. https://doi.org/10.1088/1478-7814/18/1/325
3 F. Abelès: Surf. Sci. **56** (1976) 237. https://doi.org/10.1016/0039-6028(76)90450-7
4 J. Homola, S. S. Yee, and G. Gauglitz: Sens. Actuators, B **54** (1999) 3. https://doi.org/10.1016/S0925-4005(98)00321-9
5 J. Homola: Chem. Rev. **108** (2008) 462. https://doi.org/10.1021/cr068107d
6 R. B. M. Schasfoort and A. McWhirter: "SPR instrumentation" in Handbook of Surface Plasmon Resonance, R. B. M. Schasfoort and A. J. Tudos, Eds. (RSC Publishing, Cambridge, 2008) Chap. 3. http://dx.doi.org/10.1039/9781847558220
7 S. G. Nelson, K. S. Johnston, and S. S. Yee: Sens. Actuators, B **35–36** (1996) 187. https://doi.org/10.1016/S0925-4005(97)80052-4
8 Y. H. Huang, H. P. Ho, S. Y. Wu, and S. K. Kong: Adv. Opt. Technol. **2012** (2012) 471957. https://doi.org/10.1155/2012/471957
9 S. Deng, P. Wang, and X. Yu: Sensors **17** (2017) 2819. https://doi.org/10.3390/s17122819
10 A. V. Kabashin, S. Patskovsky, and A. N. Grigorenko: Opt. Express **17** (2009) 21191. https://doi.org/10.1364/OE.17.021191
11 D. M. Wilson, S. Hoyt, J. Janata, K. Booksh, and L. Obando: IEEE Sens. J. **1** (2001) 256. https://doi.org/10.1109/7361.983465
12 Y. Huang, L. Zhang, H. Zhang, Y. Li, L. Liu, Y. Chen, X. Qiu, and D. Yu: Micromachines **11** (2020) 526. https://doi.org/10.3390/mi11050526
13 E. G. Ruiz, I. Garcés, C. Aldea, M. A. López, J. Mateo, J. Alonso-Chamarro, and S. Alegret: Sens. Actuators, A **37–38** (1993) 221. https://doi.org/10.1016/0924-4247(93)80038-I
14 Y. Liu, Q. Liu, S. Chen, F. Cheng, H. Wang, and W. Peng: Sci. Rep. **5** (2015) 12864. https://doi.org/10.1038/srep12864
15 T. Matsuda and H. Odagawa: Appl. Opt. **60** (2021) 3569. https://doi.org/10.1364/AO.420857

16 T. Inagaki, M. Motosuga, and E. T. Arakawa: Phys. Rev. B **28** (1983) 4211. https://doi.org/10.1103/PhysRevB.28.4211
17 L. Mashev and E. Popov: J. Opt. **18** (1987) 3. https://doi.org/10.1088/0150-536X/18/1/001
18 G. P. Bryan-Brown and J. R. Sambles and M. C. Hutley: J. Mod. Opt. **37** (1990) 1227. https://doi.org/10.1080/09500349014551301
19 Y. Okuno, T. Suyama, R. Hu, S. He, and T. Matsuda: Trans. Inst. Electron., Inf. Commun. Eng., Sect. E **E90-C** (2007) 1507. https://doi.org/10.1093/ietele/e90-c.7.1507
20 G. Ruffato and F. Romanato: Opt. Lett. **37** (2012) 2718. https://doi.org/10.1364/OL.37.002718
21 K. Matsubara, S. Kawata, and S. Minami: Appl. Opt. **27** (1988) 1160. https://doi.org/10.1364/AO.27.001160
22 A. A. Kolomenskii, P. D. Gershon, and H. A. Schuessler: Appl. Opt. **36** (1997) 6539. https://doi.org/10.1364/ao.36.006539
23 A. Karabchevsky, S. Karabchevsky, and I. Abdulhalim: J. Nanophotonics **5** (2011) 051813. https://doi.org/10.1117/1.3598138
24 S. K. Srivastava, R. Verma, and B. D. Gupta: Sens. Actuators, B **153** (2011) 194. https://doi.org/10.1016/j.snb.2010.10.038
25 X.-l. Zhang, Y. Liu, T. Fan, N. Hu, Z. Yang, X. Chen 1, Z.-y. Wang, and J. Yang: Sensors **17** (2017) 1435. https://doi.org/10.3390/s17061435
26 P. D. Thungon, A. Kakoti, L. Ngashangva, and P. Goswami: Biosens. Bioelectron. **97** (2017) 83. https://doi.org/10.1016/j.bios.2017.05.041
27 M. Nevièr: "The homogeneous problem," in Electromagnetic Theory of Gratings, R. Petit, Ed. (Springer, 1980) Chap. 5. https://doi.org/10.1007/978-3-642-81500-3
28 F. K. Coradin, G. R. C. Possetti, R. C. Kamikawachi, M. Muller, and J. L. Fabris: J. Microw. Optoelectron. Electromagn. Appl. **9** (2010) 131. https://doi.org/10.1590/S2179-10742010000200007
29 M. Martínez-Reina, E. Amado-González, W. Goméz-Jaramillo: J. Solution Chem. **44** (2015) 206. https://doi.org/10.1007/s10953-015-0305-5
30 R. J. Jiménez Riobóo, M. Philipp, M. A. Ramos, and J. K. Krüger: Eur. Phys. J. E **30** (2009) 19. https://doi.org/10.1140/epje/i2009-10496-4